ELSEVIER

Journal of Nuclear Materials 248 (1997) 196–203

journal of nuclear materials

Effect of grain size on recrystallization in high burnup fuel pellets

K. Nogita [a,*], K. Une [a], M. Hirai [a], K. Ito [b], K. Ito [c], Y. Shirai [d]

[a] *Nippon Nuclear Fuel Development Co., Ltd., 2163, Narita-cho, Oarai-machi, Higashi-Ibaraki-gun, Ibaraki-ken 311-13, Japan*
[b] *Hitachi, Ltd., 1-1, Saiawi-cho 3-chome, Hitachi-shi, Ibaraki-ken 317, Japan*
[c] *Toshiba Corporation, 8 Shinsugita-cho, Isogo-ku, Yokohama 235, Japan*
[d] *Tokyo Electric Power Company, 4-1 Egasaki-cho, Tsurumi-ku, Yokohama 230, Japan*

Abstract

The effect of grain size on recrystallized structure formation in the outer region of high burnup UO_2 fuel pellets was studied by optical microscopy, SEM, EPMA, XRD and TEM. Specimens were prepared from three kinds of fuels with different grain size (the standard pellet (grain size: 9 μm), the undoped large-grained pellet (51 μm) and the alumino-silicate-doped large-grained pellet (45 μm)), irradiated up to an average pellet burnup of 60 GWd/t in the Halden Reactor. The TEM observations showed that recrystallized structures were formed in a region from the middle to the edge (relative radius: $r/r_0 = 0.7–1.0$) of all fuel pellets, though they were less likely to form in the undoped large-grained pellet and the alumino-silicate-doped large-grained pellet than in the standard one. This result agreed qualitatively with the results obtained from optical microscope observations of the whole pellet region, SEM fractographs, and measurements of Xe concentration in the fuel matrix by EPMA. The effects of grain size and irradiation temperature on recrystallized structure formation were discussed in connection with fission damage accumulation. © 1997 Elsevier Science B.V.

1. Introduction

Three features of structural changes have been observed in the outermost peripheral part of high burnup pellets. They are a change to fine crystal grains, an increase in porosity, and a decrease of fission gas in the matrix (i.e., the rim structure) [1–4]. This unique microstructural change area develops with increasing burnup from the pellet edge inward to the pellet center [2]. The local burnup and temperature thresholds for the formation of this structure were estimated to be approximately above 60–70 GWd/t [5] and below 850–1100°C [6,7], respectively. Furthermore, the change in lattice parameter and TEM observation results over a wide burnup range have revealed that the mechanism of rim structure formation involves the accumulation of irradiation defects and the formation of coarsened bubbles owing to fission gas atoms being swept out from the matrix which accompanies the growth of recrystallized grains [8,9]. The sub-divided small grains were confirmed through SEM observations to correspond to the formation of recrystallized structures, and to the increased porosity caused by the formation of coarsened bubbles. Two of us previously reported the effect of grain size on microstructural change and damage recovery in UO_2 fuels irradiated to 23 GWd/t, but these fuel pellets had not recrystallized because of the lower burnup than that needed for rim structure formation [10]. Therefore, no study has been made so far on the relation between the grain size and the recrystallization of high burnup pellets. In light of this, we have examined in detail, high burnup pellets of different crystal grain sizes using optical microscopy, scanning electron microscopy (SEM), electron probe microanalysis (EPMA), X-ray diffraction (XRD) and transmission electron microscopy (TEM).

2. Experimental procedure

2.1. Fuel samples

The pellet samples used in our experiment were obtained from three kinds of UO_2 fuels with different grain

* Corresponding author. Tel.: +81-29 266 2131; fax: +81-29 266 2589; e-mail nogita@nfd.co.jp.

0022-3115/97/$17.00
PII S0022-3115(97)00156-6

sizes, irradiated up to an average pellet burnup of 60 GWd/t in the Halden Reactor (a Norwegian test reactor). These were the standard pellet (grain size: 9 μm), the undoped large-grained pellet (51 μm) and the 0.25 wt%-alumino-silicate-doped large-grained pellet (45 μm). The standard pellet was fabricated by sintering in a reducing atmosphere. The undoped large-grained pellet was sintered in an oxidizing atmosphere which enhances cation diffusivity and grain growth. The alumino-silicate-doped pellet had a large grain structure due to the additive forming a liquid phase during sintering which enhanced diffusivity in grain boundaries. Almost all doped alumino-silicate precipitated on the grain boundaries, and alumino-silicate-doping had little effect on fuel behavior [11]. All pellets had 13% enrichment and a small diameter of 5.5 mm, which allows rapid burnup accumulation. The zircaloy cladding tubes had a small diameter (outer diameter: 6.53 mm, inner diameter: 5.61 mm) and a Zr-liner with a thickness of 50 μm. At full reactor power, the average linear heat rate of the rods was kept at about 290–390 W/cm. More detailed information on this pellet, the rod design, and irradiation history were described elsewhere [11]

2.2. Examinations

After optical microscope observations of a pellet cross section as-etched, a fracture surface, which was prepared by a diamond scratch technique, was observed in detail by SEM across the pellet radius.

Elemental analyses of fission products, which were retained in the fuel sample, were carried out using a shielded EPMA. The measurement conditions were as follows: acceleration voltage, 20 kV; electron beam current, 200 nA; beam diameter, 30 μm.

The XRD measurements of the fuel samples in their pellet outer region were made using a shielded diffractometer with Ni-filtered Cu K_α radiation. The accelerating voltage and current were 40 kV and 30 mA, respectively. The diameter of the X-ray beam was 1.0 mm. The lattice parameter was obtained by least-squares calculations of the five diffraction lines between 90° and 130° in 2θ. The error in the lattice parameter was less than ± 0.1 pm.

The samples for TEM were prepared by an ion milling technique [9]. Small cubic pieces of pellets with cladding, about 1 mm on each side, were obtained from each pellet at the radial location of the fuel periphery using a cross cutter. The TEM specimens were embedded in inorganic cement within a 3 mm diameter stainless steel washer and ground to a thickness of about 100 μm. Then, a dimple was made on the edge of the pellet using a dimple grinder. The thinning process was completed by ion micromilling with 5 keV argon ions. The thickness of the TEM observation area was about 40–100 nm. The TEM observation area for determination of recrystallization ratio, as described in Fig. 6, was approximately 10×10 μm.

3. Results and discussion

3.1. Optical and SEM observations

Fig. 1 show ceramograph and SEM fractographs of the standard pellet. Crack patterns can be seen in the ceramograph, which was considered to be formed during power down. A dark ceramographic zone was found between the periphery and the middle portion and a similar feature appeared in ceramographs of the other fuels. SEM images of fracture surfaces in Fig. 1a–c correspond to the position of (a) central, (b) middle and (c) peripheral regions of the ceramograph of the standard pellet. The peripheral region in Fig. 1c indicates the presence of a sub-divided grain structure, i.e., a rim structure, as seen in commercial fuels irradiated to high burnup [1–4]. It is a noticeable point that the middle region of Fig. 1b also shows the sub-divided structure. This suggests that the dark ceramographic zone was related to the rim structure. Other fuels also showed a similar sub-divided structure in the middle portion. Fig. 2a, b show the fracture surfaces in the periphery for the undoped and the alumino-silicate-doped large-grained pellets. The standard pellet (Fig. 1c) has a more developed sub-divided grain structure compared with the undoped (Fig. 2a) and the alumino-silicate-doped large-grained (Fig. 2b) pellets.

3.2. EPMA measurements

The radial distribution of Xe retained in the matrix of the three fuels, which were measured by EPMA, are shown in Fig. 3. The concentration of Xe was normalized by that of U. This figure also shows the generated Xe profile which was calculated by using the Ce profile [4]. This generated Xe profile is almost flat, except for about a 5–10% enhanced concentration close to the pellet rim ($r/r_0 = 0.96$–1.0). This effect is attributable to the neutronic rim effect (Pu buildup by epithermal neutron captures of ^{238}U), though the gradient of the peripheral region is remarkably lower than that of commercial pellets.

The concentration of Xe shows a significant release from the central to middle regions ($r/r_0 = 0$–0.6) of all the pellets. This indicates higher Xe atom mobility at higher irradiation temperatures in this portion. On the other hand, Xe concentration profiles in the middle to the peripheral regions ($r/r_0 = 0.6$–1.0) at lower irradiation temperatures with its lower atomic and bubble mobility, show significant differences in the three pellets. Variation of Xe concentration in this portion is closely related to the formation of rim structure [12]. According to the formation mechanism of rim structure reported by us [9], the newly formed coarsened bubbles in the pellet peripheral region are interpreted as formed by sweeping out of fission gas atoms and small intragranular bubbles during grain growth on recrystallization and to contain almost all the swept-out

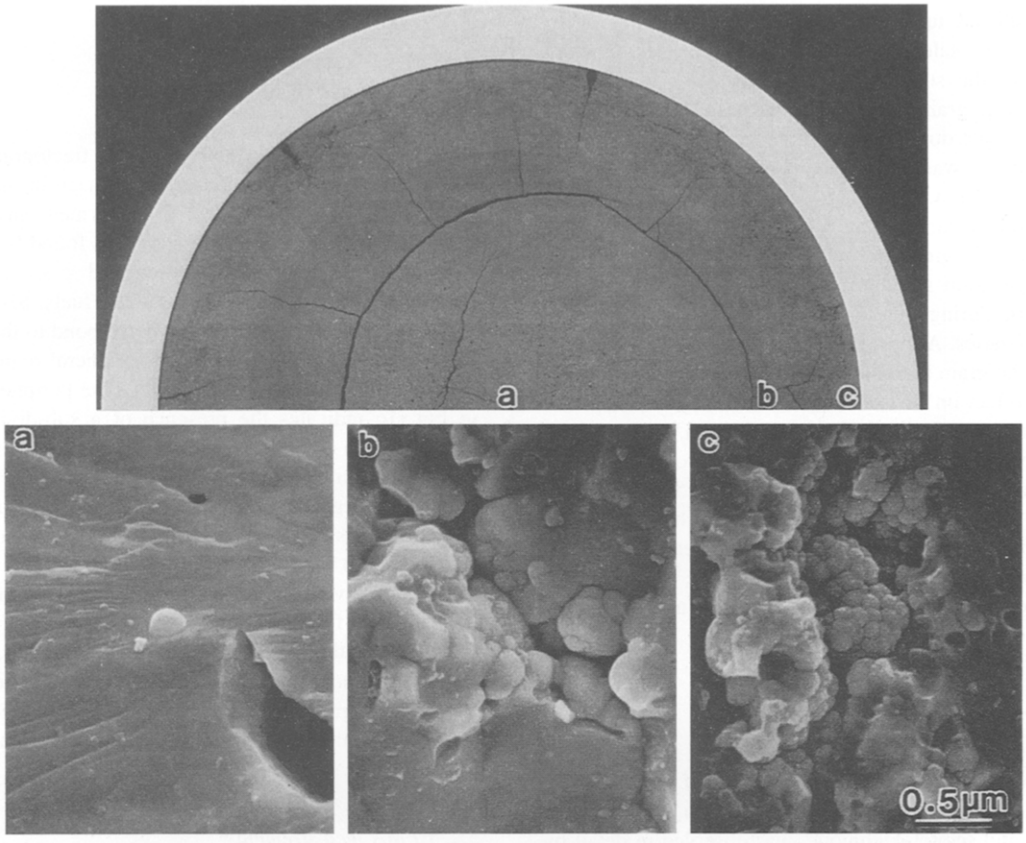

Fig. 1. Ceramograph and SEM fractographs of standard pellet; (a) central, (b) middle, and (c) peripheral regions.

gases in the rim bubbles at high pressure. A depletion of the Xe concentration in the rim structure region should have resulted from the lowering of EPMA sensitivity for the Xe enclosed in larger bubbles [12]. Therefore, the depletion of Xe from the generated amount in the portion of $r/r_0 = 0.6$–1.0 is defined as fractional fission gas retention in the rim bubbles; i.e., the coarsened bubbles. The shaded region in Fig. 3 corresponds to the fractional

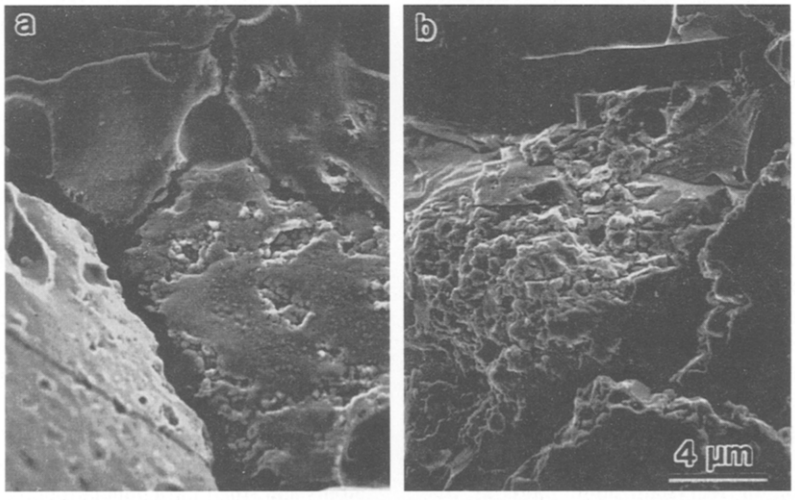

Fig. 2. SEM fractographs of peripheral region; (a) undoped large-grained pellet, (b) alumino-silicate-doped large-grained pellet.

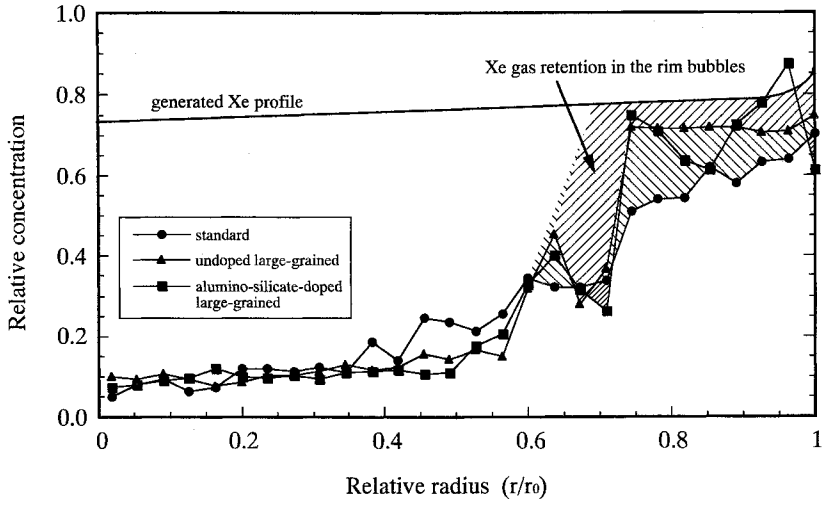

Fig. 3. Radial distributions of Xe concentration.

fission gas retention. These values are 18% for the standard, 10% for the undoped large-grained and 11% for the alumino-silicate-doped large-grained pellets.

3.3. XRD measurements

Fig. 4 shows the lattice parameter increase for the standard, undoped and alumino-silicate-doped large-grained pellets in the outer region, compared with that for fuels irradiated to a burnup of 34 GWd/t in the same Halden Reactor. The increase is defined as the difference between the measured lattice parameter and one corrected for the effect of FP solution, which is expressed by the following formula [13]:

$$a(\mathrm{pm}) = 547.02 - 0.0127B,$$

where a is the corrected lattice parameter and B is the burnup in GWd/t. The lattice parameter for the irradiated fuels changes with accumulation of the irradiation induced point defects and soluble FPs, and with change of oxygen to metal (O/M) ratio [7,10]. The O/M of fuels is little changed by irradiation under LWR conditions [7,14]. Then the lattice parameter increase is mainly attributable to the accumulation of irradiation defects. From the previous discussions on point defect kinetics in irradiated UO_2 fuels for high burnups (> 1 GWd/t) [7,10], these point defects are assumed to be vacancies. The standard pellet shows a larger increase in lattice parameter, compared with the undoped and the alumino-silicate-doped large-grained pellets when irradiated to 34 GWd/t, which is in good agreement with the data of 23 GWd/t fuels in Ref. [10]. The lattice parameter increase is almost the same for the all pellets when irradiated to 60 GWd/t. After the accumulation of irradiation induced vacancies reaches a saturation level, the excess vacancies would contribute to formation of the FP gas bubbles [4,8,9]. These point defect accumulations are thought to be closely related to the recrystallized grain growth, as discussed below.

3.4. TEM observations

Fig. 5a, b show bright-field TEM images of the standard and the undoped large-grained pellets in their periphery ($r/r_0 = 0.95$–1.0). There are three different characteristic microstructures in the same bright-field image of all pellets. They are accumulated damage clusters of dislocations and small intragranular bubbles, recrystallized grains, and coarsened bubbles. A similar microstructure is observed in the alumino-silicate-doped large-grained pellets. We also observed an as-fabricated grain boundary of the alumino-silicate-doped large-grained pellets, where the

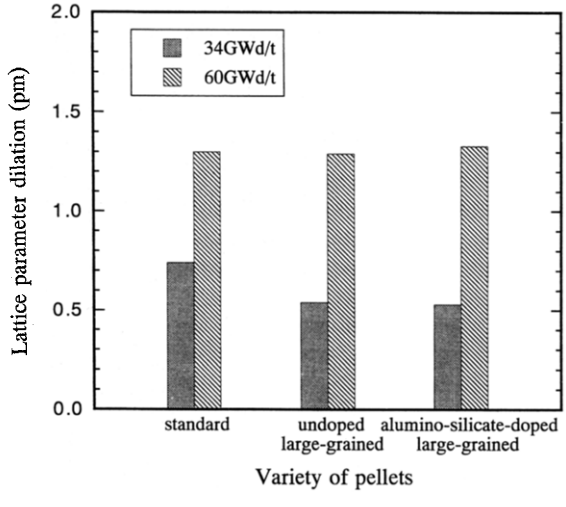

Fig. 4. Lattice parameter dilation determined by X-ray diffractometry.

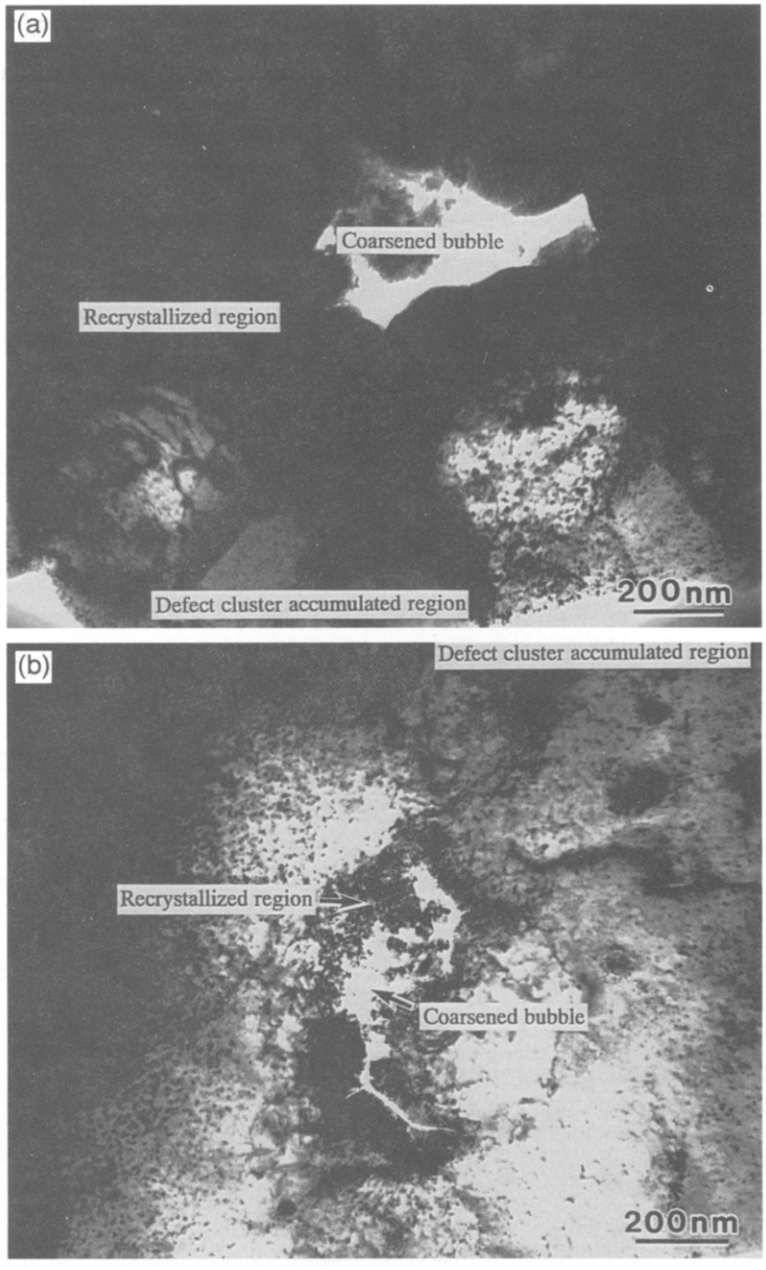

Fig. 5. Bright-field TEM images: (a) standard pellet (peripheral region); (b) undoped large-grained pellet (peripheral region).

doped alumino-silicate is precipitated. There is no doped effect on microstructural change at grain boundary. The morphology of the present recrystallized grain structure is almost the same as reported by us [9] and Thomas et al. [14]. The rim structure formation is directly related to the accumulation of radiation damage. Tangled dislocation networks are formed by the inhomogeneous accumulation of dislocations after the development of interstitial-type dislocation loops. On the other hand, intragranular FP gas bubbles are formed by the clustering of vacancies and fission gases of Kr and Xe. With increasing burnup, tangled dislocations are organized into sub-divided grains with high angle boundaries. Then, some of them are recrystallized, sweeping out small intragranular bubbles [8,9]. In Fig. 5b, some recrystallized grains surrounding the coarsened bubble are too small to be distinguished from sub-divided grains with high angle boundaries. These small grains appear to be nucleus grains for recrystallization as observed in Ref. [8].

Furthermore, in the case of the undoped large-grained

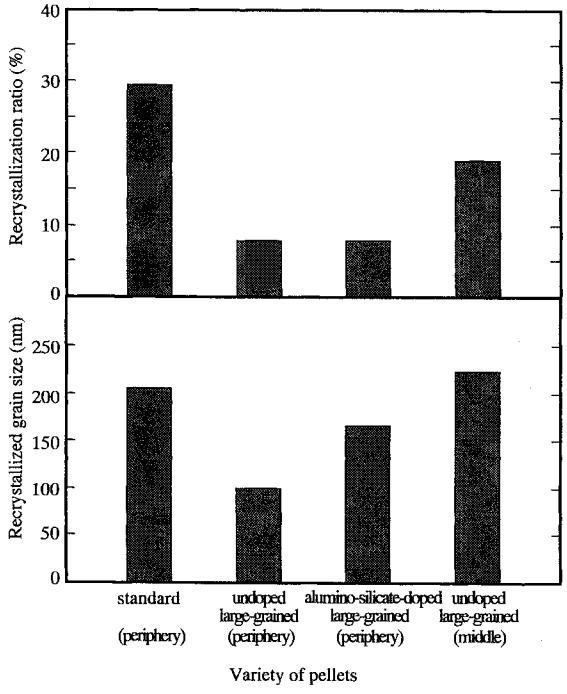

Fig. 6. Recrystallization ratio and average recrystallized grain size of pellets.

fuel, TEM observation was also made on the middle region ($r/r_0 = 0.7$) of the pellet radius location. This area corresponds to the dark ring shown by optical microscopy and the sub-divided structure by SEM fractograph. Coarsened rim bubbles and recrystallized grains are found, whose features are nearly the same as those in the peripheral region of this pellet.

Fig. 6 shows the recrystallization ratio (the ratio of recrystallized structure in the total TEM observation area, excluding coarsened bubbles) and recrystallized grain size of each pellet in the peripheral and the middle regions of the undoped large-grained pellet. The observed area for determination of recrystallization ratio and recrystallized grain size is approximately 10×10 μm and data are obtained from the dark-field image [9]. These values in the periphery are 30% and 205 nm for the standard pellet, 8% and 100 nm for the undoped large-grained pellet, and 8% and 166 nm for the alumino-silicate-doped large-grained pellet, respectively. As a reference, these values for a commercial BWR pellet (local burnup: 100 GWd/t) are 40% and 170 nm, respectively [9]. Recrystallized structures are less likely to form in the undoped large-grained pellet and the alumino-silicate-doped large-grained pellet than in the standard pellet. This result agrees qualitatively with the results obtained from ceramography, fracture SEM images and the measurement of the Xe concentration in the fuel matrix by EPMA. Furthermore, the recrystallization ratio and grain size at the middle region of the undoped large-grained pellet are 19% and 223 nm, which are larger than those for the peripheral region in the same undoped large-grained pellet. This indicates that the recrystallization was more developed in the middle region than in the periphery.

3.5. Discussion on recrystallization process

For recrystallization to develop, the presence of 'nucleus' grains with high-angle grain boundaries and sufficient driving forces for 'nucleus' grain growth are required. As discussed in our previous paper [9], in the case of the rim structure for high burnup UO_2 fuel, the sub-divided grains with high-angle boundaries of 20–30 nm in size [8], which are formed by inhomogeneous accumulation of dislocations, are regarded as the 'nuclei' for recrystallization. The driving force for the 'nucleus' grain growth would be supplied by strain energy of point defects and defect clusters in the matrix [9,15,16]. In this section, we discuss the effect of the grain size and the irradiation temperature on the recrystallization in connection with fission damage accumulation.

3.5.1. Formation of 'nuclei' for recrystallization

The 'nucleus' grains for recrystallization, i.e., sub-divided grains with high-angle grain boundaries, have been shown by systematic dislocation density measurements [8] to form at densities above $5–6 \times 10^{14}$ m/m^3. The reported dislocation densities on standard (grain size: 16 μm) and large-grained (43 μm) pellet peripheries, which had been irradiated to 23 GWd/t in the Halden Reactor, were 2.0×10^{14} m/m^3 and 1.8×10^{14} m/m^3, respectively [10]. From this result, we concluded that no grain size effect on microstructural change was recognized up to the burnup of 23 GWd/t. Therefore, the number of 'nucleus' grains formed inside as-fabricated grains is presumed to be the same in the standard and the large-grained pellets in the case of the extrapolated burnup of 60 GWd/t. In contrast to the inside of an as-fabricated grain, the grain boundary, which inhibits climbing motion of dislocations, is considered to be an important area for inhomogeneous dislocation accumulation. In other words, if a higher density of dislocation is accumulated near and/or on the grain boundary, a smaller grain size leads to a higher dislocation density since there is a larger grain boundary surface area per volume. The conditions of the original as-fabricated grain boundary area are not clear in the present work, though we reported one important aspect previously [4]. In that paper, the TEM image of the 83 GWd/t pellet showed that a high density of dislocations decorated the as-fabricated grain boundary. Furthermore, the SEM results of PWR (grain size: 4.5–6 μm) and BWR (12 μm) irradiated pellets (burnup: 42–48 GWd/t) reported by Billaux et al. [17] suggested that the cauliflower structure (sub-divided structure) developed from the grain surface

inward into the grain. They concluded that the kinetics of development of a rim structure would thus be faster in a smaller grain fuel. These reported results support inhomogeneous accumulation of dislocations near and/or on the grain boundary, as do our results for the recrystallization ratio for the three pellets.

3.5.2. Growth of 'nucleus' grains

Sufficient driving force for 'nucleus' grain growth to 100–200 nm sizes is required for recrystallization. This driving force is brought about by strain energy of point defects of vacancy and/or vacancy-FP complex [9,15,16] accumulated in the matrix. The lattice dilation is mainly due to the accumulation of fission-induced vacancies. In Fig. 4, lattice parameter dilations for the three pellets are already saturated and show essentially the same value for the 60 GWd/t burnup samples, though the lattice parameter of the standard pellet is certainly higher than that of the undoped and the alumino-silicate-doped large-grained pellet for 34 GWd/t. From the point defect kinetics in homogeneous solids during irradiation [12], vacancy concentration, C_v, is represented by $C_v \propto C_s^{1/2} \propto (1/r)^{1/2}$, where C_s is the sink density and r, the grain radius. This indicates more fission-induced vacancies, which supply grain growth energy, accumulate in the lattice of the standard pellet than in the large-grained one.

Irradiation temperature is also an important factor for grain growth. The recrystallization ratio and the grain size of the middle region in the undoped large-grained pellet are larger (19%, 223 nm) than those in the peripheral region (8%, 100 nm). Since the irradiation temperature is higher in the middle region than in the periphery, once 'nucleus' grains are formed by inhomogeneous accumulation of dislocations, growth of 'nucleus' grains is easily progressed in the middle region. However, irradiation-induced point defects, which are directly related to the formation of 'nucleus' grains for recrystallization and supplying grain growth energy, are recovered during irradiation in the higher temperature region such as the pellet center region. In the out-of-pile annealing experiment of irradiated pellets [7], point defects were completely recovered at temperature above 850°C for 5 h. Of course this threshold temperature of 850°C would be somewhat underestimated when considering the actual situation of simultaneous recovery and nucleation of point defects. Below this threshold temperature, a higher temperature is favored for recrystallized grain growth. In the case of our pellets irradiated in the Halden Reactor, the distribution of point defects in the matrix is supposed to be flat in the region at temperatures below the recovery threshold temperature (the middle to peripheral region) since the burnup profile is almost flat. Therefore, the recrystallization progresses more prominently in the middle region than in the periphery. For a commercial LWR case, recrystallization initially occurs at the periphery even at lower temperature because local burnup at this region is much higher (about 2–2.5 times) than the pellet average. Thus the recrystallization is expected to progress in the middle portion for further irradiation.

4. Conclusions

From optical microscopy, SEM, EPMA, XRD and TEM results of the standard pellet (grain size: 9 μm), the undoped large-grain pellet (51 μm) and the alumino-silicate-doped large-grained pellet (45 μm) irradiated to an average pellet burnup of 60 GWd/t, the following conclusions were obtained.

Optical microscope and SEM images of all pellets indicated the presence of a sub-divided grain structure at peripheral region and middle region of pellet radial location. The radial distribution of Xe retained in the matrix measured by EPMA showed a significant Xe release at the portion from the central to middle regions of all the pellets, while in the middle to peripheral regions there were significant differences in them. The fractional Xe retention (the depletion of Xe from the generated amount in the region of $r/r_0 = 0.6–1.0$), which must be one of the rim structure formation indices, had values of 18% for the standard, 10% for the undoped large-grained and 11% for the alumino-silicate-doped large-grained pellets. The lattice parameter increase was almost the same for all the pellets. TEM images for all the pellets of periphery and middle regions indicated the presence of (a) accumulated defect clusters of dislocations and small intragranular bubbles, (b) recrystallized grains, and (c) coarsened bubbles. The recrystallization ratio (the ratio of recrystallized structure in the total TEM observation area, excluding coarsened bubbles) and recrystallized grain size were 30% and 205 nm for the standard pellet (periphery), 8% and 100 nm for the undoped large-grained pellet (periphery), 19% and 223 nm for same pellet (middle region), and 8% and 166 nm for the alumino-silicate-doped large-grained pellet, respectively.

From the above detailed examination results, it was concluded that the large grain pellet suppressed the recrystallization (and following rim structure formation), which was considered due to the small accumulation of irradiation induced defects.

References

[1] Hj. Matzke, H. Blank, M. Coquerelle, K. Lassmann, I.L.F. Ray, C. Ronchi, C.T. Walker, J. Nucl. Mater. 166 (1989) 165.

[2] R. Manzel, R. Eberle, Proc. ANS Topical Meeting on LWR Fuel Performance, Avignon, Apr. 1991, p. 528.

[3] M.E. Cunningham, M.D. Freshley, D.D. Lanning, J. Nucl. Mater. 188 (1992) 19.

[4] K. Une, K. Nogita, S. Kashibe, M. Imamura, J. Nucl. Mater. 188 (1992) 65.

[5] K. Lassmann, C.T. Walker, J. van de Laar, F. Lindström, J. Nucl. Mater. 226 (1995) 1.
[6] T. Kameyama, T. Matsumura, M. Kinoshita, Nucl. Technol. 106 (1994) 334.
[7] K. Nogita, K. Une, J. Nucl. Sci. Technol. 30 (1993) 900.
[8] K. Nogita, K. Une, Nucl. Instrum. Methods B91 (1994) 301.
[9] K. Nogita, K. Une, J. Nucl. Mater. 226 (1995) 302.
[10] K. Nogita, K. Une, J. Nucl. Sci. Technol. 31 (1994) 929.
[11] R. Yuda, H. Harada, M. Hirai, T. Hosokawa, K. Une, S. Kashibe, S. Shimizu, T. Kubo, these Proceedings, p. 262.
[12] M. Mogensen, C. Bagger, C.T. Walker, J. Nucl. Mater. 199 (1993) 85.
[13] K. Une, M. Oguma, J. Nucl. Mater. 74 (1978) 290.
[14] Hj. Matzke, J. Nucl. Mater. 208 (1994) 18.
[15] L.E. Thomas, C.E. Beyer, L.A. Charlot, J. Nucl. Mater. 188 (1992) 80.
[16] J. Rest, G.L. Hofman, J. Nucl. Mater. 210 (1994) 187.
[17] M.R. Billaux, L.F. van Swan, S.H. Shann, Proc. ANS Topical Meeting on LWR Fuel Performance, West Palm Beach, FL, Apr. 1994, p. 242.